

Conduction in Relaxation-Case Semiconductors

G. H. Döhler and H. Heyszenau

Max-Planck-Institut für Festkörperforschung, D 7 Stuttgart-1, Federal Republic of Germany

(Received 21 March 1973)

It is shown that the diffusion term cannot be neglected in the differential equations governing the relaxation case, even in the high-field limit. We present quantitative results of rigorous calculations including diffusion. Good agreement with experiments is obtained for reverse bias, including the typical sublinear region. In forward direction a superlinear region is found in disagreement with previous predictions of "recombinative space-charge injection."

Drastic deviations from familiar semiconductor behavior arise once the dielectric relaxation time $\tau_D = \epsilon/4\pi\sigma$ exceeds the minority-carrier diffusion-length lifetime τ_0 .^{1,2} This inequality, $\tau_D > \tau_0$, defines the "relaxation case" which is of great practical importance as it is realized in low-conductivity materials³ and is assumed to be valid for amorphous alloys.⁴ The suggestion has even been made that threshold switching is to be explained that way.⁴ General conclusions have been derived by van Roosbroeck and co-workers¹⁻³ from linearized approximations to the nonlinear system of differential equations governing transport in this regime. In giving these explanations, several approximations were made in Ref. 2 which, in particular, include neglecting the diffusion current in regions of high electric field. In this Letter we report the first quantitative results of rigorous calculations. It is shown that neglect of diffusion for forward bias leads to false conclusions even in the high-field limit, whereas the reverse-bias behavior¹⁻³ is confirmed.

In the relaxation case, a common electrochemical potential $\varphi_n(x) = \varphi_p(x) = \varphi(x)$ governs the respective electron and hole densities $n(x)$ and $p(x)$ also with an external bias applied.^{1,2} Hence, the rate equation for free-carrier generation and recombination may be replaced by the equilibrium condition $n(x)p(x) = n_i^2 = \text{const}$. We assume equal electron and hole mobilities $\mu_n = \mu_p = \mu$ and equal effective masses. This puts the intrinsic Fermi level $\psi(x)$ at midgap,

$$\psi(x) = \frac{1}{2}[E_c(x) + E_v(x)]. \quad (1)$$

The two differential equations governing the relaxation regime assume an especially simple form in terms of $\varphi(x)$ and $\psi(x)$.

(1) Poisson's equation, which gives the curva-

ture of the bands, can be written

$$\partial^2\psi/\partial x^2 = 8\pi e^2 n_i \epsilon^{-1} \{ \sinh[\beta(\varphi - \psi)_0] - \sinh[\beta(\varphi(x) - \psi(x))] \} \quad (2)$$

in the case of no trapping [$\beta = (kT)^{-1}$].

(2) Continuity for the total steady-state current density j (the sum of electron and hole contributions to field and diffusion currents) demands

$$\frac{\partial\varphi}{\partial x} = \left(\frac{\partial\varphi}{\partial x} \right)_{x_c} \{ \cosh[\beta(\varphi(x) - \psi(x))] \}^{-1}. \quad (3)$$

The driving force $\partial\varphi/\partial x$ attains its maximum

$$(\partial\varphi/\partial x)_{x_c} = j(2n_i\mu)^{-1} \quad (4)$$

at the *conversion point* x_c ,¹⁻³ defined by $\varphi(x_c) = \psi(x_c)$. There the conductivity goes through its minimum $\sigma_{\min} = 2n_i\mu e$, and changes from n to p type. A conversion point is always present in a sufficiently long specimen with one minority-carrier-injecting electrode. Detailed inspection of Eqs. (2) and (3),⁵ as well as the numerical evaluations outlined below, indicate a broadening of the zone with nearly *minimum conductivity*¹⁻³ upon increasing a reverse bias. For samples of finite length this broadening causes a sublinear voltage dependence of the current. Similar qualitative conclusions were found earlier with neglect of diffusion.^{1,2}

Forward bias, however, narrows this low-conductivity zone with increasing voltage. A proof will be given later⁵ that diffusion in this case always dominates near x_c , even in the limit of high fields. Three characteristic predictions of Ref. 2, leading to remarkable consequences for the current-voltage relation of finite samples, turn out to be artifacts of an inadmissible approximation, namely, replacing $\partial\varphi/\partial x$ by the electric field $(\partial\psi/\partial x)_{x_c}$, thus ignoring diffusion:

(a) The local field $(\partial\psi/\partial x)_{x_c}$ is actually lower,

and not—as claimed²—much higher than that far away from the electrode.

(b) No space-charge zone of majority carriers appears, as indicated in Fig. 3 of Ref. 2. Such space charge was postulated for matching the “high-field region” near x_c to the “low-field region” in the unmodulated bulk.²

(c) The width of the carrier depletion zone in the vicinity of x_c decreases with increasing bias, while it was asserted² to increase. Thus, a superlinear region in the forward current-voltage relation follows, resembling space-charge-limited currents.⁶ The predicted² sublinear current dependence, related to “recombinative space-charge injections,”² cannot be derived from the basic Eqs. (2) and (3) alone, but requires additional mechanisms such as velocity saturation, special trapping conditions, or current-limiting contacts. This point requires further research for a complete interpretation of the experimentally observed sublinear characteristics in semi-insulating GaAs for forward bias.^{3,6}

Numerical results obtained by integrating (2)

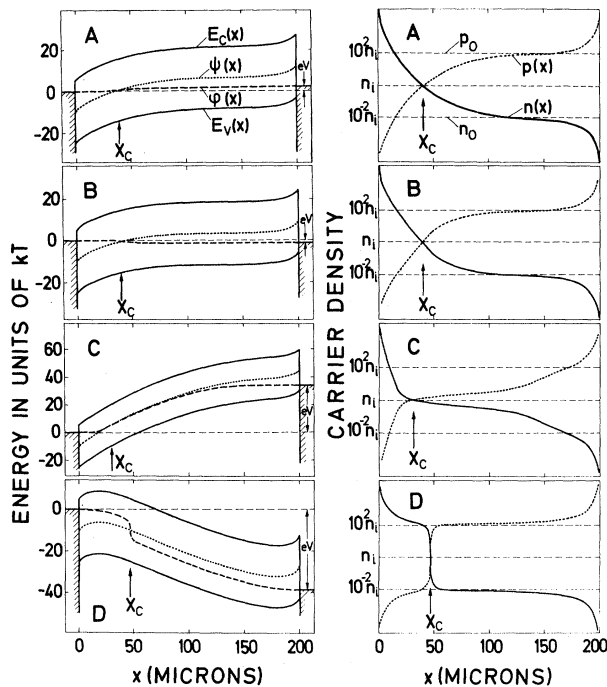


FIG. 1. (a) Potential profiles of relaxation-case structure defined in text. Solid lines, band edges E_c and E_v ; dotted lines, intrinsic Fermi level $\psi(x)$; dashed lines, electrochemical potential $\phi(x)$; x_c is the “conversion point” (see text), eV the applied bias. A, C reverse bias; B, D forward, as shown in Fig. 2. (b) Corresponding electron (solid lines) and hole (dashed) densities on a logarithmic scale.

and (3) simultaneously are represented in Fig. 1 for a p -type relaxation-case semiconductor of length $L = 2 \times 10^{-2}$ cm, with $n_i = 4 \times 10^8$ cm⁻³, $p_0 = 10^2 n_i$, $n_0 = 10^{-2} n_i$ at room temperature, and $\epsilon = 10$. The contact on the left is assumed to be n injecting with $\phi(0) - \psi(0) = 10kT$; the other one p injecting, with $\phi(L) - \psi(L) = -10kT$. The plots in Figs. 1(a) and 1(b) pertain to the points A · · · D indicated on the current-voltage characteristic Fig. 2. Figure 1(a) shows the electrochemical potential $\phi(x)$ (dashed line), the intrinsic Fermi level $\psi(x)$ (dotted), and parallel to it the conduction- and valence-band edges $E_c(x)$ and $E_v(x)$ (solid lines). Figure 1(b) gives the logarithm of the corresponding densities of electrons (solid lines) and holes (dashed). For low reverse (case A) as well as forward bias (case B) almost all the voltage drop appears in the vicinity of x_c (arrows), and hence the sample behaves like a thin specimen of intrinsic material with constant resistance. In particular, this resistance is largely independent of doping of the electrode material (as long as one of them is n injecting and the other p injecting) and even of the length of the sample.⁵ The curves for C show the widening of the nearly intrinsic region upon increasing reverse bias, which causes the sublinear region in the current-voltage characteristic. For very high reverse bias the current-voltage curve approaches that for an intrinsic sample of the same

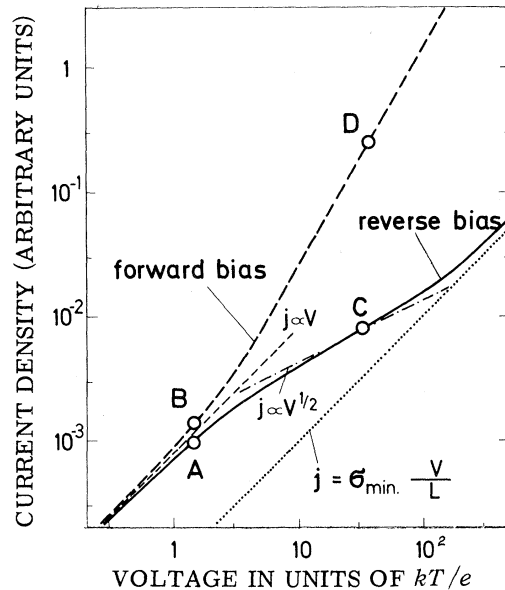


FIG. 2. Current density j versus voltage V for forward bias (dashed line) and reverse bias (solid line). The points A to D of Fig. 1 are shown. Dotted line, current-voltage relation for the corresponding sample of “minimum conductivity” (see text).

length (dashed line in Fig. 2). Case *D* finally shows the situation at high forward bias. Here the substantial difference between our results and the ones given earlier² becomes evident by comparing our plots for case *D* with Fig. 3 of Ref. 2.

The present examples selected from our calculations demonstrate well the general features of relaxation-case materials. Consequences for the interpretation of measurements on amorphous materials will be discussed subsequently⁵ with particular reference to the range of validity of the relaxation-case concepts.

We thank Professor W. Brenig and Professor H. J. Queisser for many valuable discussions. We are especially indebted to Professor H. J.

Queisser for having stimulated our interest in this subject.

¹W. van Roosbroeck and H. C. Casey, Jr., in *Proceedings of the Tenth International Conference on the Physics of Semiconductors*, Cambridge, Massachusetts, 1970, edited by S. P. Keller, J. C. Hensel, and F. Stern, CONF-700801 (U. S. AEC Division of Technical Information, Springfield, Va., 1970), p. 832.

²W. van Roosbroeck and H. C. Casey, Jr., *Phys. Rev. B* **5**, 2154 (1972).

³H. J. Queisser, H. C. Casey, Jr., and W. van Roosbroeck, *Phys. Rev. Lett.* **26**, 551 (1971).

⁴W. van Roosbroeck, *Phys. Rev. Lett.* **28**, 1120 (1972).

⁵G. H. Döhler and H. Heyszenau, to be published.

⁶A. P. Ferro and S. K. Ghandhi, *J. Appl. Phys.* **40**, 4015 (1972).

Molecular-Beam Study of Hydrogen-Deuterium Exchange on Low- and High-Miller-Index Platinum Single-Crystal Surfaces*

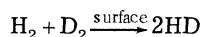
S. L. Bernasek,† W. J. Siekhaus, and G. A. Somorjai

Inorganic Materials Research Division, Lawrence Berkeley Laboratory, and Department of Chemistry, University of California, Berkeley, California 94720

(Received 12 April 1973)

The hydrogen-deuterium exchange reaction takes place readily on a platinum single crystal with high Miller index (997), but not detectably on a platinum single crystal of low Miller index (111). The difference in reactivity is ascribed to the large density of atomic steps present on the high-index surface that are responsible for the dissociation of the diatomic molecules.

The dissociation of hydrogen on solid surfaces is an initial step in many important surface reactions.¹ Hydrogen dissociation can be conveniently studied by monitoring the hydrogen-deuterium exchange reaction



taking place in the presence of the surface. The scattering of a mixed hydrogen-deuterium molecular beam from the solid surface can be a particularly useful technique to investigate the surface-dissociation mechanism of hydrogen.

Molecular-beam scattering studies have shown that this exchange reaction takes place readily on Ni(111) and Pt(111) oriented thin films.^{2,3} Classical studies have shown that the reaction takes place readily on a variety of polycrystalline solid surfaces.⁴ On the other hand, the formation of HD, indicating hydrogen dissociation, was not readily detected during molecular-beam scattering studies from the (100) single crystal face

of platinum.⁵ It is apparent from these contradictory results that the polycrystalline and thin-film surfaces contain surface sites that are responsible for dissociation, while the single-crystal surface does not. In order to verify the nature of surface sites where dissociation of the hydrogen molecules occurs, we have studied the hydrogen-deuterium exchange on the (111) face of platinum and on the (997) high-Miller-index face of platinum. This high-Miller-index face is characterized by an ordered arrangement of atomic steps (of one atom height) separated by atomic terraces of (111) orientation and nine atoms wide.⁶ The two crystal faces differ only in the density of atomic steps.

A schematic diagram of the experimental apparatus⁷ is shown in Fig. 1. The incident molecular beam is modulated by a variable-frequency chopper and then scattered from the crystal surface, whose surface geometry and chemical composition are monitored by low-energy electron